

# 1 *EraSOR: Erase Sample Overlap in* 2 *polygenic score analyses*

3 Shing Wan Choi <sup>1,2\*</sup>, Timothy Shin Heng Mak <sup>3</sup>, Clive J. Hoggart <sup>1</sup>, Paul F. O'Reilly <sup>1,2</sup>

4       1 Department of Genetics and Genomic Sciences, Icahn School of Medicine, Mount Sinai, 1  
5 Gustave L. Levy Pl, New York City, NY 10029, USA;

6       2 MRC Social, Genetic and Developmental Psychiatry Centre, Institute of Psychiatry,  
7 Psychology and Neuroscience, King's College London, De Crespigny Park, Denmark Hill,  
8 London, UK, SE5 8AF; and

9       3 Centre of Genomic Sciences, University of Hong Kong, 21 Sassoon Road, Pokfulam, Hong  
10 Kong SAR, China

11       \*To whom correspondence should be addressed

## 12 **Abstract**

## 13 **Background**

14 Polygenic risk score (PRS) analyses are now routinely applied in biomedical research, with great hope  
15 that they will aid in our understanding of disease aetiology and contribute to personalized medicine. The  
16 continued growth of multi-cohort genome-wide association studies (GWASs) and large-scale biobank  
17 projects has provided researchers with a wealth of GWAS summary statistics and individual-level data  
18 suitable for performing PRS analyses. However, as the size of these studies increase, the risk of inter-  
19 cohort sample overlap and close relatedness increases. Ideally sample overlap would be identified and  
20 removed directly, but this is typically not possible due to privacy laws or consent agreements. This  
21 sample overlap, whether known or not, is a major problem in PRS analyses because it can lead to inflation  
22 of type 1 error and, thus, erroneous conclusions in published work.

## 23 **Results**

24 Here, for the first time, we report the scale of the sample overlap problem for PRS analyses by generating  
25 known sample overlap across sub-samples of the UK Biobank data, which we then use to produce GWAS  
26 and target data to mimic the effects of inter-cohort sample overlap. We demonstrate that inter-cohort  
27 overlap results in a significant and often substantial inflation in the observed PRS-trait association,  
28 coefficient of determination ( $R^2$ ) and false-positive rate. This inflation can be high even when the absolute  
29 number of overlapping individuals is small if this makes up a notable fraction of the target sample. We  
30 develop and introduce EraSOR (Erase Sample Overlap and Relatedness), a software for adjusting  
31 inflation in PRS prediction and association statistics in the presence of sample overlap or close  
32 relatedness between the GWAS and target samples. A key component of the EraSOR approach is  
33 inference of the degree of sample overlap from the intercept of a bivariate LD score regression applied to  
34 the GWAS and target data, making it powered in settings where both have sample sizes over 1,000  
35 individuals. Through extensive benchmarking using UK Biobank and HapGen2 simulated genotype-

36 phenotype data, we demonstrate that PRSs calculated using EraSOR-adjusted GWAS summary statistics  
37 are robust to inter-cohort overlap in a wide range of realistic scenarios and are even robust to high levels  
38 of residual genetic and environmental stratification.

39 **Conclusion**

40 The results of all PRS analyses for which sample overlap cannot be definitively ruled out should be  
41 considered with caution given high type 1 error observed in the presence of even low overlap between  
42 base and target cohorts. Given the strong performance of EraSOR in eliminating inflation caused by  
43 sample overlap in PRS studies with large (>5k) target samples, we recommend that EraSOR be used in all  
44 future such PRS studies to mitigate the potential effects of inter-cohort overlap and close relatedness.

45 **Introduction**

46 Polygenic risk scores (PRSs) are proxies of individuals' genetic liability to a trait or disease [1] that have  
47 been applied in numerous research settings, including patient stratification [2] and investigation of  
48 treatment response [3–6]. The power of PRS analyses is dependent on the heritability and polygenicity of  
49 the trait, the power of the genome wide association study (GWAS) used to derive the PRS, and the size of  
50 the target data sample [7]. The recent surge of high quality genetic and phenotypic data from large-scale  
51 biobank projects, such as the UK Biobank [8], BioBank Japan [9], Taiwan Biobank [10], and FinnGen  
52 [11], as well as GWAS resources from large consortia such as the Psychiatric Genomic Consortium  
53 (PGC) [12], GIANT [13] and the Global Lipids Genetics Consortium (GLGC) [14] have provided  
54 unprecedented opportunity to perform highly-powered PRS analyses.

55 However, expansion in data size does not come without a cost in this setting: as sample sizes increase,  
56 there is greater risk that samples are recruited into multiple cohorts or that entire cohorts are included in  
57 multiple consortia. For PRS analyses, which typically test for association between PRS and a trait(s) or  
58 outcome of interest, overlapping samples between the GWAS and target data samples can result in  
59 spurious inflation of the coefficient of determination ( $R^2$ ) and association  $P$ -values, leading to false-  
60 positive and exaggerated findings [15]. Overlapping samples should ideally be removed from either the  
61 GWAS or target data to avoid misinterpretation of results, but participant privacy agreements usually  
62 limit access to raw genotyping data, meaning that this is generally not an option.

63 Here we first evaluate the extent to which different degrees of sample overlap and relatedness between  
64 GWAS and target samples generates biased PRS-trait associations. Next, to overcome the sample overlap  
65 problem, we develop and introduce EraSOR (Erase Sample Overlap and Relatedness), a python software  
66 that adjusts GWAS summary statistics [1] to correct for inflation of PRS-trait association results caused  
67 by overlapping samples between the GWAS and target samples. Through extensive simulations using the  
68 UK Biobank genetic data [8], we demonstrate that EraSOR can robustly adjust for inflation in test  
69 statistics caused by various degrees of overlapping samples, level of relatedness, or ascertainment  
70 schemes in case/control settings. We propose that EraSOR will increase the accuracy of results in all  
71 future PRS studies with known sample overlap and will act as a sensitivity tool for assessing the  
72 reliability of results in PRS studies with unknown but potential sample overlap. EraSOR is an open-  
73 source software and is freely available at <https://gitlab.com/choishingwan/EraSOR>.

74

75

76 **Methods**

77 **EraSOR framework**

78 Consider two GWAS  $k = \{1, 2\}$  performed on the same continuous outcome  $Y_k$ . The effect size of the  $g^{\text{th}}$   
 79 SNP in study  $k$  ( $\beta_{kg}$ ) is estimated using a regression model

$$Y_k = \alpha_{kg} + \beta_{kg} X_{kg} + \varepsilon_{kg} \#(1)$$

80

81 where  $X_{kg}$  is the standardized genotype vector for SNP  $g$  in study  $k$ , and  $\varepsilon_{kg}$  is the random error assumed  
 82 to be independent between studies. Under the null model of no contribution of SNP  $g$  to the trait,  $\beta_{kg} =$   
 83 0, and assuming no sample overlap, then  $\widehat{\beta}_{1g}$  and  $\widehat{\beta}_{2g}$  estimated from the two GWASs should be  
 84 independent, i.e.,  $\text{cor}(\widehat{\beta}_{1g}, \widehat{\beta}_{2g}) = 0$ . However, when there are overlapping samples between the two  
 85 studies, then a correlation is induced between the regression coefficients, such that  $\text{cor}(\widehat{\beta}_{1g}, \widehat{\beta}_{2g}) \neq 0$ .  
 86 From LeBlanc et al [16], this correlation can be approximated as

$$\text{cor}(\widehat{\beta}_{1g}, \widehat{\beta}_{2g}) \approx \frac{N_c}{\sqrt{N_1 N_2}} \text{cor}(Y_1, Y_2) \#(2)$$

87 for quantitative traits, where  $\text{cor}(Y_1, Y_2)$  represents the correlation between the traits;  $N_c$  is the number of  
 88 overlapping samples; and  $N_1, N_2$  are the sample sizes of studies 1 and 2, respectively [16]. Since we are  
 89 considering only a single phenotype here,  $\text{cor}(Y_1, Y_2)$  is equal to 1, and so we have:

$$\text{cor}(\widehat{\beta}_{1g}, \widehat{\beta}_{2g}) \approx \frac{N_c}{\sqrt{N_1 N_2}} \#(3)$$

90 which captures correlations only due to sample overlap independent of the true causal effect. Assuming  
 91 sample overlap does not affects the standard error estimates, LeBlanc et al [16] proposed that when the  
 92 number of overlapping samples ( $N_c$ ) is known, one can adjust the joint distribution of the summary  
 93 statistics (z-scores) of the two GWASs as:

$$\mathbf{z}_{\text{de-corr}} = \mathbf{C}^{-0.5} \mathbf{z} \#(4)$$

94 where  $\mathbf{z}$  is a 2-by- $M$  matrix containing z-scores estimated in each study,  $M$  is the number of SNPs  
 95 common to both studies, and  $\mathbf{C}$  is the 2x2 matrix with ones on its diagonal and  $\text{cor}(\widehat{\beta}_{1g}, \widehat{\beta}_{2g})$  as its off-  
 96 diagonal elements. While this adjustment is effective [16], it requires prior knowledge of  $N_c$ , which is  
 97 typically unknown in PRS studies. However, we propose utilizing univariate and bivariate LD score  
 98 regression [17,18] to estimate  $\frac{N_c}{\sqrt{N_1 N_2}}$  and thus  $\text{cor}(\widehat{\beta}_{1g}, \widehat{\beta}_{2g})$  from Eq. 3 as follows:

100 Bivariate LD score regression is typically used to estimate the genetic correlation between two traits using  
 101 the GWAS corresponding to each, and is defined in [13] by the following equation:

$$\mathbb{E}[z_{1j} z_{2j}] = \frac{\sqrt{N_1 N_2} \rho_g}{M} l_j + \frac{N_c \rho}{\sqrt{N_1 N_2}} + \rho_g F_{ST}^2 \sqrt{N_1 N_2} + \frac{N_c^2 F_{ST} \sigma_s^2}{\sqrt{N_1 N_2}} \#(5)$$

103 where  $l_j$  is the LD score of SNP  $j$ ;  $\rho_g$  is the genetic covariance between the two traits;  $\rho = \rho_g + \rho_e$ ;  $\rho_e$   
 104 is the non-genetic covariance;  $F_{ST}$  and  $\sigma_s$  are the genetic and environmental stratification respectively.

105 LDSC assumes two underlying populations within each cohort, and that the levels of genetic and  
 106 environmental stratification are similar in the two cohorts, e.g.  $F_{ST}^{(1)} \approx F_{ST}^{(2)} = F_{ST}$  and  $\sigma_{S1} \approx \sigma_{S2} = \sigma_S$   
 107 [13]. Since we are considering only a single phenotype here,  $\rho$  is equal to 1, and so we have:

$$108 \quad \mathbb{E}[z_{1j}z_{2j}] = \frac{\sqrt{N_1N_2}\rho_g}{M}l_j + \frac{N_c}{\sqrt{N_1N_2}} + \rho_g F_{ST}^2 \sqrt{N_1N_2} + \frac{N_c^2 F_{ST} \sigma_S^2}{\sqrt{N_1N_2}} \#(6)$$

109 We wish to solve for  $N_c$  and hence apply Eq. 3 to generate a de-correlated base GWAS that does not lead  
 110 to inflated PRS-trait associations due to sample overlap. To do this, we will utilize the univariate LD  
 111 score regression model. The univariate LD score regression equation can be derived as a special case of  
 112 the bivariate LD score equation by assuming that the two outcomes and cohorts are identical [13,17],  
 113 leading to:

$$\mathbb{E}[\chi_j^2] = \frac{Nh^2}{M}l_j + 1 + NF_{ST}(h^2 F_{ST} + \sigma_S^2) \#(7)$$

114 Univariate LD score regression performs a regression of observed  $\chi^2$  on  $l_j$ , with the effect size estimate of  
 115  $l_j$  corresponding to a scaled estimate of heritability ( $\widehat{h}_i^2$ ) and with the estimated intercept term,  $\widehat{l}_u$  as  
 116 follows:

$$\widehat{l}_u = 1 + N_i F_{ST} \left( \widehat{h}_i^2 F_{ST} + \sigma_S^2 \right)$$

117 If we assume that the environmental stratification  $\sigma_S^2 = 0$ , then we have:

$$\begin{aligned} \widehat{l}_u &= 1 + N_i F_{ST} \left( \widehat{h}_i^2 F_{ST} + \sigma_S^2 \right) \\ \widehat{l}_u &= 1 + N_i F_{ST}^2 \widehat{h}_i^2 \\ F_{ST}^2 &= \frac{\widehat{l}_u - 1}{N_i \widehat{h}_i^2} \end{aligned} \#(8)$$

118 Since we can estimate  $F_{ST}^2$  using both the base and target data, we then take the weighted mean estimate  
 119 of both:

$$\widehat{F}_{ST}^2 = \frac{1}{N_1 + N_2} \sum_{i=1}^2 \frac{\widehat{l}_i - 1}{\widehat{h}_i^2} \#(9)$$

120 The intercept term of the bivariate LD score regression is:

$$\widehat{l}_b = \frac{N_c}{\sqrt{N_1N_2}} + \widehat{\rho}_g F_{ST}^2 \sqrt{N_1N_2} + \frac{N_c^2 F_{ST} \sigma_S^2}{\sqrt{N_1N_2}} \#(10)$$

121 Substituting Eq. 9 and  $\sigma_S^2 = 0$  into Eq. 10, we have:

$$\begin{aligned} \widehat{l}_b &= \frac{N_c}{\sqrt{N_1N_2}} + \widehat{\rho}_g \widehat{F}_{ST}^2 \sqrt{N_1N_2} + \frac{N_c^2 F_{ST} \sigma_S^2}{\sqrt{N_1N_2}} \\ \widehat{l}_b &= \frac{N_c}{\sqrt{N_1N_2}} + \widehat{\rho}_g \sqrt{N_1N_2} \left( \frac{1}{N_1 + N_2} \sum_{i=1}^2 \frac{\widehat{l}_i - 1}{\widehat{h}_i^2} \right) \end{aligned}$$

$$\hat{I}_b = \frac{N_c}{\sqrt{N_1 N_2}} + \frac{\hat{\rho}_g \sqrt{N_1 N_2}}{N_1 + N_2} \sum_{i=1}^2 \frac{\hat{I}_i - 1}{\hat{h}_i^2} \#(11)$$

122 Since we can estimate the genetic covariate ( $\hat{\rho}_g$ ), the trait heritability  $\hat{h}_i^2$  and the intercepts from the  
123 univariate and bivariate LD score regression analyses of the GWAS and target data, we can obtain an  
124 estimate of  $\frac{N_c}{\sqrt{N_1 N_2}}$ . Substituting this estimate into Eq. 3 will derive an estimate of  $\text{cor}(\hat{\beta}_{1g}, \hat{\beta}_{2g})$  that can  
125 be used to produce de-correlated GWAS z-statistics via Eq.4. EraSOR automatically performs the  
126 bivariate LD score and univariate LD score regression analyses on the GWAS summary statistics  
127 generated from the base and target data. To test the performance of EraSOR, including its robustness to  
128 the modelling assumptions (e.g., assuming  $\sigma_S^2 = 0$ ), we performed a series of extensive simulations.

## 129 **UK Biobank genotype data**

130 The UK Biobank is a prospective cohort study of around 500,000 individuals recruited across the United  
131 Kingdom during 2006-2010. The genetic data from UK Biobank comprises 488,377 samples and 805,426  
132 SNPs. Standard quality control (QC) procedures were performed, removing any SNPs with minor allele  
133 frequency  $< 0.01$ , genotype missingness  $> 0.02$  and with a Hardy Weinberg Equilibrium Test  $P$ -value  $<$   
134  $1 \times 10^{-8}$ . Samples with high levels of missingness or heterozygosity, with mismatching genetic-inferred and  
135 self-reported sex, or with aneuploidy of the sex chromosomes were removed as recommended by the UK  
136 Biobank data processing team. Next, 4-means clustering was applied to the first two Principal  
137 Components (PCs) of the genotype data and those individuals in the (largest) cluster corresponding to  
138 European ancestry were retained for the primary analyses because polygenic risk scores have been shown  
139 to have low portability between ancestries [14] motivating ancestry-matched PRS studies until cross-  
140 ancestry PRS methods are developed, which our main results correspond to (see section *Samples with*  
141 *population stratification* below, which describes analyses that we also performed on individuals of all  
142 ancestries in the UK Biobank). A greedy algorithm [19] was then used to remove related individuals, with  
143 kinship coefficient  $> 0.044$ , in a way that maximized sample retention. In our simulations that investigate  
144 the effect of related individuals in the GWAS and target data, we instead randomly retain one first degree  
145 relative (defined as kinship coefficient  $\geq 0.177$  and  $\leq 0.354$ ) of a randomly sampled individual in the  
146 GWAS data. Altogether, we retain 557,369 SNPs, 387,392 individuals and 23,429 of their first-degree  
147 relatives for the set of analyses performed. For the simulations of population stratified samples, we  
148 extracted samples 10 standard deviations from the centroid of the European cluster and defined these as  
149 “non-European” samples. Quality control procedures were repeated using the parameters described above  
150 after combining these non-European samples with the European samples, resulting in 387,365 samples of  
151 European ancestry and 21,779 individuals of non-European ancestry. Code used to perform the QC and  
152 corresponding documentation are available at [https://choishingwan.gitlab.io/ukb-administration/admin/master\\_generation/](https://choishingwan.gitlab.io/ukb-administration/admin/master_generation/). This research has been conducted using the UK Biobank  
153 Resource under application 18177 (Dr O'Reilly).

155

156

157

158

159

160 ***Phenotype simulation***

161 ***Quantitative Traits without population structure***

162 Quantitative phenotypes ( $Y$ ) with heritability ( $h^2$ ) of 0, 0.1, and 0.5 were simulated using the UK Biobank  
163 genotype data (post QC; see above) as input. Quantitative traits were simulated as:

$$Y = (\alpha + X\beta + \varepsilon)\delta \#(12)$$

164 where  $X$  is the standardized genotype matrix corresponding to all samples and 10,000 randomly  
165 selected SNPs with effect size  $\beta$  following a standard normal distribution.  $X\beta$  were adjusted such that it  
166 has mean 0 and variance of  $h^2$ ; and  $\varepsilon$  represents the random error, which follows  $\varepsilon \sim N(0, \sqrt{1 - h^2})$ . To  
167 ensure EraSOR works for distribution that are not only standard normal, we included  $\alpha$  as the phenotypic  
168 mean randomly sampled from a normal distribution with mean 0 and standard deviation of 1, and  $\delta$  as the  
169 phenotypic variable randomly sampled from 1 to 100 to simulate phenotypes that does not follow the  
170 standard normal distribution.

171 To model polygenic risk score analyses with sample overlap, we randomly selected either 120k or 250k  
172 individuals from the sample of 387,392 individuals available to us (see above) to generate two different  
173 sizes of base GWAS data. Next, we randomly sampled 1,000, 5,000 or 10,000 individuals from the  
174 remaining sample to act as three different sizes of target data, of which 0%, 5%, 10%, 50% or 100% were  
175 randomly selected from the base data sample so that there was a known degree of sample overlap between  
176 the base and target data. In addition, we generated an “overlap-free” base cohort in which the overlapping  
177 samples were removed from the base cohort so that we could compare the result of applying EraSOR  
178 against results of physically removing overlapped samples from the base cohort.

179 In order to search a feasible parameter space in sufficient depth, we only simulate phenotype with  
180 heritability of 0.5, with a base cohort of 250k and target cohort of 5,000; only simulate base cohort with  
181 120k samples when the phenotypic heritability is  $\leq 0.1$  and target cohort has 5,000 samples; and only  
182 simulate target cohort with 1,000 and 10k samples when the base cohort contain 250k samples and the  
183 phenotypic heritability is  $\leq 0.1$ . The entire set of simulations were repeated 100 times.

184 ***Binary Trait***

185 Binary traits were simulated under the liability threshold model [20], simulating a normally distributed  
186 liability using Eq. 12 with  $\alpha = 0$ ,  $\delta = 1$ , and cases defined as samples with disease liability higher than  
187 liability thresholds of 0.9, 0.7 and 0.5, corresponding to population prevalences of 0.1, 0.3 and 0.5,  
188 respectively. To limit the complexity of our simulations, the sample prevalence of our cohorts follows the  
189 population prevalence.

190 In the binary trait setting, overlap can be ascertained such that the overlap is among cases, or among  
191 controls, or among both. To investigate the effect of case-only or control-only overlap, we randomly  
192 selected 120k effective samples (effective samples defined as  $N_{eff} = 4/(1/N_{cases} + 1/N_{controls})$  [21])  
193 as the base cohort, and then randomly selected 5,000 effective samples as the target cohort, where 0%,  
194 5%, 10%, 30% or 50% of the cases or of the controls in the target cohort were sampled from the base  
195 cohort. We also performed simulations where the overlapping samples were selected at random among  
196 cases and controls. An “overlap-free” base cohort was generated with all overlapping samples removed.

197 In order to search a feasible parameter space in sufficient depth, we only vary the trait heritability when  
198 the population prevalence is 0.1, and only vary the population prevalence when the trait heritability is  $\leq$   
199 0.1. These simulations were repeated 100 times.

200 **Related samples**

201 Spurious inflation in PRS analysis test statistics may also be observed when there are closely related  
202 individuals between the base and target cohorts. To investigate the effects of relatedness on PRS results,  
203 we repeated the quantitative trait simulations with a modified Eq. 12:

$$Y = (\alpha + X\beta + \theta + \epsilon)\delta \#(13)$$

204 where  $\theta$  is the shared environment between the related individuals and follows a random normal  
205 distribution with mean 0 and variance  $\sigma_\theta^2 \in (0, 0.3, 0.6)$  if and only if  $\sigma_\theta^2 + h^2 < 1$ , with each related pair  
206 of individuals having the same  $\theta$  value.  $\epsilon$  represents a combination of non-shared environment and  
207 random error, which follows  $\epsilon \sim N\left(0, \sqrt{1 - h^2 - \sigma_\theta^2}\right)$ . To model the inter-cohort relatedness, we first  
208 select all individuals with a first-degree relative in the UK Biobank (kinship coefficient  $\geq 0.177$  and  $\leq$   
209 0.354), of which there are 23,429 individuals, and then randomly select additional samples who do not  
210 have any first-degree relatives to form a base cohort containing 250k samples. We then generate target  
211 cohorts containing 5,000 samples, with either 0%, 30%, 60% or 100% of the target samples being first-  
212 degree relatives of samples in the base cohort. We also generated a reference cohort from the base cohort  
213 where all the related samples in the target cohort were replaced by unrelated individuals for  
214 benchmarking the performance of EraSOR. The entire set of simulations were repeated 100 times.

215 **Samples with population stratification**

216 An assumption of the EraSOR algorithm is that the environmental stratification ( $\sigma_s^2$ ) is zero. When  
217 environmental stratification is present,  $\frac{N_c^2 F_{ST} \sigma_s^2}{\sqrt{N_1 N_2}}$  from Eq. 10 is no longer 0 and a bias proportional to the  
218 environmental stratification and the genetic stratification ( $F_{ST}$ ) may be introduced. We devised two  
219 strategies for simulating data with both environmental and genetic stratification to test the sensitivity of  
220 EraSOR to deviations of each from 0. In the first, we partitioned the UK Biobank into European and non-  
221 European ancestries, while in the second we used the simulation software HapGen2 [22].

222 In the first simulation strategy, the UK Biobank samples were divided into European and non-European  
223 ancestries based on 4-mean clustering on PC1 and PC2 (see above). Quantitative traits with  
224 environmental stratification were then simulated as:

$$Y = (\alpha + X\beta + S + \epsilon)\delta \#(12)$$

225 with the environmental stratification term (S) defined as

$$S = \begin{cases} -\sqrt{\frac{\sigma_s^2}{2}}, & \text{Non-European Ancestry} \\ \sqrt{\frac{\sigma_s^2}{2}}, & \text{European Ancestry} \end{cases}$$

226 where  $\sigma_S^2$  can take a value of 0, 0.3 or 0.9 if and only if  $\sigma_S^2 + h^2 < 1$ , and  $\epsilon$  represents the residual  
227 term, which follows  $\epsilon \sim N\left(0, var(X\beta + S - 2cov(X\beta, S)) \sqrt{\frac{1-h^2-\sigma_S^2}{h^2+\sigma_S^2}}\right)$ , with  $cov(X\beta, S)$  being the  
228 covariance between  $X\beta$  and  $S$ . To investigate the effect of sample overlap in the presence of  
229 environmental and genetic stratification, we randomly selected either 120k or 250k individuals from the  
230 sample of 409,144 individuals available to us (see above) to generate two different sizes of base GWAS  
231 data. Next, we randomly sampled 5,000 or 10,000 individuals from the remaining sample to act as two  
232 different sizes of target data, of which 0%, 10%, 50% or 100% were randomly selected from the base data  
233 sample. To ensure that the genetic and environmental stratification is the same within the base and target  
234 data, the same ancestry ratio was maintained in all simulated data sets, matching the ratio in the full data  
235 set (~5% non-European ancestry). In addition, we generated an “overlap-free” base cohort in which the  
236 overlapping samples were removed from the base cohort to allow benchmarking the performance of  
237 EraSOR. The entire set of simulations were repeated 25 times.

238 Given that only ~5% of the UK biobank samples correspond to individuals of non-European ancestry, the  
239 effect of genetics and environmental stratification may be limited. Thus, we developed a second strategy  
240 to test their effects in which we used HapGen2 [22] to simulate 180k Yoruban and 180k Finnish samples  
241 using recombination maps from the 1000 Genomes Project [23]. 500 “Finnish” samples and 500  
242 “Yoruban” samples were selected to calculate the LD scores using LDSC (v1.0.1) and flashPCA (v2.0)  
243 [24] was used to calculate the first 15 PCs of the data.

244 We repeated the population stratification simulation using the HapGen2 simulated genotype data, with  $S$   
245 represented now segregate according to the simulated population. The entire set of simulations were  
246 repeated 25 times.

## 247 ***Genome Wide Association Study and Polygenic Score Analysis***

248 Genome wide association analyses (GWAS) were performed on the base and target cohorts using PLINK  
249 2.0 (version 2021-08-04) [25] with the  $--glm$  function. As binary traits were only simulated for the  
250 European ancestry only analyses, where population structure was not simulated, and considering the  
251 computational cost of including covariates in the logistic regression, we did not include PCs in our binary  
252 trait analysis. On the other hand, quantitative traits were simulated in all scenarios, some of which are  
253 population stratified. Thus, we included 15 PCs as a covariate for our quantitative trait analyses. The  
254 resulting summary statistics were then provided to EraSOR to generate the adjusted summary statistics  
255 using European LD scores [17] calculated from 1,000 Genomes Project Phase 3 data [23] or the LD  
256 scores calculated from a subset of the simulated genotypes (HapGen2 simulation) using LDSC (v1.0.1)  
257 [17]. PRS analyses using the adjusted, unadjusted, and the “overlap-free” summary statistics were  
258 performed using PRSice-2 (v2.3.5) [26] with the default settings. The  $R^2$  and  $P$ -value of association of the  
259 PRS-trait tests were reported.

## 260 ***Strategy for Benchmarking***

261 To investigate the level of spurious inflation caused by inter-cohort relatedness and overlapped samples,  
262 we first established a baseline PRS  $R^2$ , calculated using base cohorts without overlapped samples. The  
263 bias can then be measured as the observed PRS  $R^2$  minus the baseline PRS  $R^2$  ( $\Delta R^2$ ), given the same  
264 phenotype and cohort sizes. For non-heritable traits, we also measure the level of false-positive, defined  
265 as any PRS with  $P$ -value  $< 1 \times 10^{-4}$  [27].

266 On the other hand, to compare the performance of EraSOR with the optimal strategy of directly removing  
267 overlapping samples – an option that is typically not available – we calculate PRSs: (i) using summary  
268 statistics adjusted by EraSOR (“adjusted PRS”) and (ii) using summary statistics generated from a base  
269 cohort with all overlapping and/or related samples removed (“overlap-free PRS”). We present the  
270 performance of EraSOR as the PRS-trait association  $R^2$  of the adjusted PRS minus the  $R^2$  of the  
271 overlap-free PRS ( $\Delta R^2$ ). If EraSOR has successfully corrected for the sample overlap, then  $\Delta R^2$  should  
272 be close to 0.

273 **Results**

274 ***Inflation caused by overlap***

275 The presence of overlapping samples between the base and target data sets is known to cause inflated  
276 association between polygenic risk scores (PRS) and phenotypes [15], but the extent and characteristics of  
277 the problem have not been described. Here, we performed extensive simulations using the UK Biobank  
278 [8] genotype data to investigate the inflation caused by different levels and types of inter-cohort sample  
279 overlap in relation to traits simulated with varying heritability and prevalence (see Methods). Base and  
280 target cohorts were generated with varying degrees of sample overlap, measured as  $\frac{N_c}{\sqrt{N_1 N_2}}$ , where  $N_c$  is  
281 the number of overlapping samples and  $N_1$  and  $N_2$  are the sample sizes of the base and target cohort,  
282 respectively. PRS analyses were conducted using the standard *clumping+thresholding* (C+T) PRS  
283 calculation method [1], implemented in *PRSice* [26].

284 We first estimated the false-positive rate induced by sample overlap by simulating non-heritable traits and  
285 recording the fraction of significant PRS-trait association (Supplementary Fig. 1). Highly significant  
286 associations between PRS and non-heritable phenotypes were observed when even limited inter-cohort  
287 sample overlap was present (Fig. 1). Specifically, for non-heritable quantitative traits, the inflation in  
288 association (e.g. *p*-value of association) is highly positively correlated with the degree of overlap (Pearson  
289 Correlation coefficient ( $\gamma$ ) = 0.96, *P*-value < 2.2x10<sup>-16</sup>). For example, when there is a base cohort of 250k  
290 samples, target cohort of 5,000 samples and 250 overlapping samples (5% of target sample; degree of  
291 overlap = 0.0071) the false positive rate is 17%, while this increases to 94% when there are 500  
292 overlapping samples (10% of target sample; degree of overlap = 0.014) (Fig 1a).

293

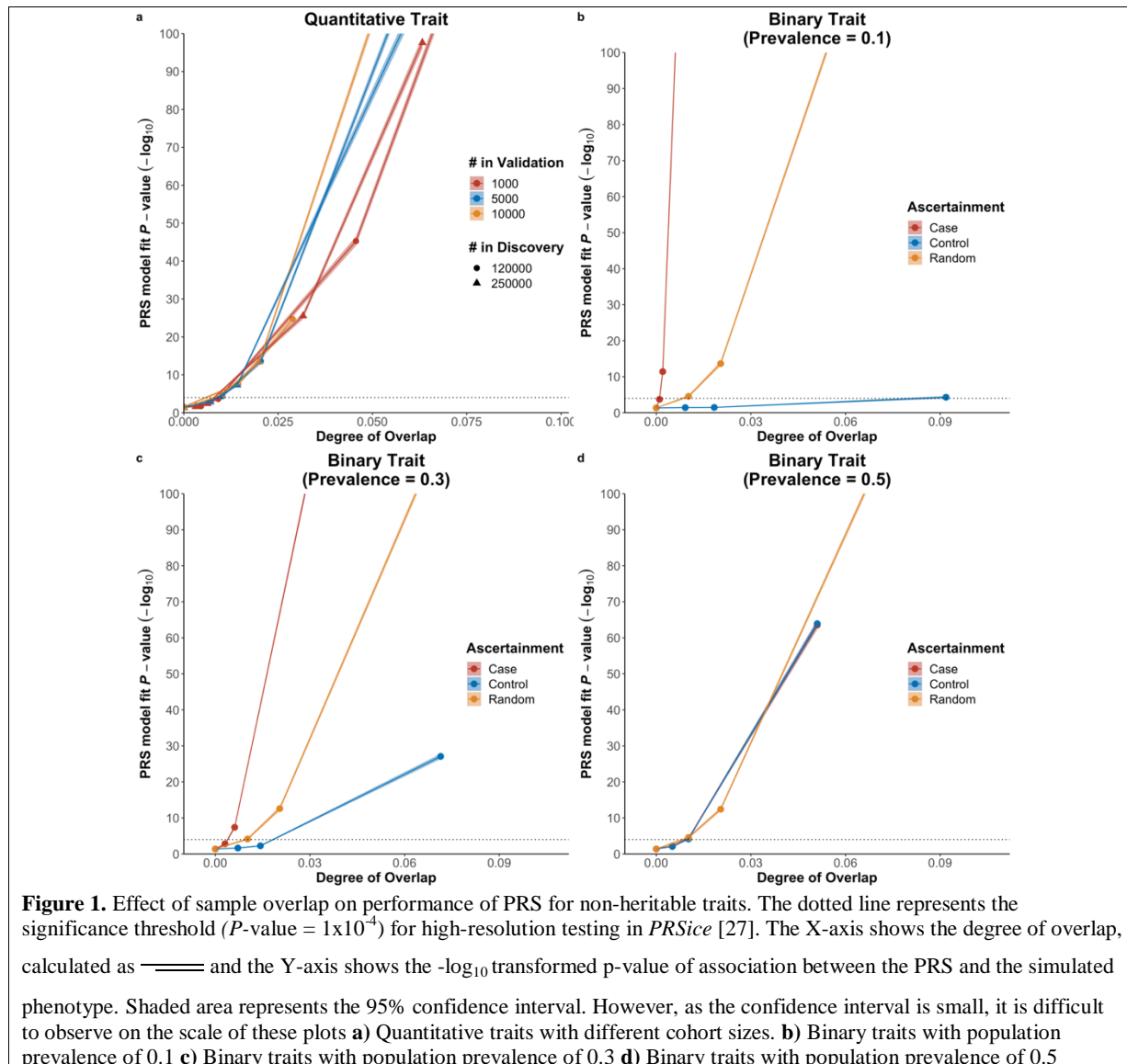


**Figure 1.** Effect of sample overlap on performance of PRS for non-heritable traits. The dotted line represents the significance threshold ( $P$ -value =  $1 \times 10^{-4}$ ) for high-resolution testing in PRSice [27]. The X-axis shows the degree of overlap, calculated as  $\frac{\text{Number of overlapping individuals}}{\text{Total number of individuals}}$  and the Y-axis shows the  $-\log_{10}$  transformed  $P$ -value of association between the PRS and the simulated phenotype. Shaded area represents the 95% confidence interval. However, as the confidence interval is small, it is difficult to observe on the scale of these plots **a**) Quantitative traits with different cohort sizes. **b**) Binary traits with population prevalence of 0.1 **c**) Binary traits with population prevalence of 0.3 **d**) Binary traits with population prevalence of 0.5

294

295 In the binary trait setting, sample overlap may be among cases only, controls only, or be among both. 296 These alternatives were investigated by first simulating binary traits with different population prevalence 297 using the liability threshold model [20]. Cohorts with effective sample sizes of 120k in the base data and 298 5000 in the target data were generated with different degrees and scenarios of sample overlap. We 299 observed extreme inflation associated with case-only overlap when population prevalence is lower than 300 0.5. For a binary trait with population prevalence 0.1, a false positive rate of 43% is observed when the 301 degree of overlap is 0.001, which corresponds to 5% of the cases from the target cohort also present in the 302 base cohort (Fig 1b). When the degree of sample overlap is doubled (~0.002), the false positive rate is 303 100%. The inflation in PRS-trait association is not as sensitive to control-only sample overlap when the 304 population prevalence is small. We observe a false positive rate of ~47% when the degree of overlap is as 305 high as 0.092, which corresponds to 50% of the controls from the target cohort also present in the base 306 cohort (Fig 1b). This discrepancy between the effect of case and control overlap is a result of the 307 differential contribution of cases and controls to the PRS-trait association in our simulations. Cases are 308 sampled from the extreme upper tail of the liability distribution at a frequency corresponding to the

309 disease prevalence, which is typically low: this gives each case greater weight in the calculation of the  
310 PRS-trait association and, thus, an overlapping case will generate greater inflation than an overlapping  
311 control. This was consistent with our simulation results (Fig 1c, 1d), where the inflation in  $\Delta R^2$  caused by  
312 overlapping cases decreases as population prevalence increases ( $\gamma = -0.068$ ,  $P$ -value =  $4.70 \times 10^{-5}$ ). The  
313 reverse relationship between inflation and population prevalence was observed for control-only overlap  
314 ( $\gamma = 0.20$ ,  $p$ -value =  $3.90 \times 10^{-34}$ ). For a population prevalence of 0.5, case-only and control-only overlap  
315 have the same impact on the inflation (Fig 1d).

316 Given that complete overlap of individuals in the base and target data can generate PRS-trait associations  
317 that are severely inflated, closely related individuals independently enrolled into the base and target  
318 cohorts may induce some inflation considering their shared genetics and environment. Here we tested the  
319 effect of relatedness between the base and target cohorts on PRS-trait associations in non-heritable traits  
320 in a similar way to that for sample overlap (see Methods), where inter-cohort relatedness is defined as  
321  $\frac{N_r}{\sqrt{N_1 N_2}}$  where  $N_r$  is the number of samples in the target cohort that are first degree relatives with samples  
322 in the base cohort. A false positive rate of 76% is observed when the inter-cohort relatedness is 0.085 and  
323 the shared environment explains 30% of the trait variance (250k base, 5k target, 60% of target samples  
324 have 1<sup>st</sup> degree relatives in the base), while a false positive rate of 84% is observed with an inter-cohort  
325 relatedness of 0.042 for traits with shared environment contribution of 60% (30% related samples). See  
326 Supplementary Fig. 2 for full results regarding the effects of inter-cohort relatedness on PRS-trait  
327 association inflation.

328 In the next section we extend these investigations to consider the effects of sample overlap on PRS-trait  
329 associations on heritable traits, but we present these findings in conjunction with results based on the  
330 application of our method EraSOR, which is designed to resolve the problem.

### 331 ***Performance of EraSOR***

332 To tackle the problem of inflation caused by inter-cohort overlap and relatedness, we developed the Erase  
333 Sample Overlap and Relatedness (EraSOR) method. Using GWAS summary statistics generated from the  
334 base and target cohorts, EraSOR implements univariate and bivariate LD score regression [17,18] to  
335 estimate several parameters that are then used to perform a de-correlation calculation of the base GWAS  
336 test statistics (see Methods). These adjusted base GWAS summary statistics can then be used for  
337 downstream PRS analyses, with sample overlap or relatedness corrected for.

338 In order to evaluate the performance of EraSOR, we conducted an extensive set of simulations covering a  
339 range of scenarios of inter-cohort sample overlap and relatedness (see below and Methods).

### 340 ***Simulations using UK Biobank data***

341 We observed that for both quantitative and binary traits, EraSOR almost entirely eliminates the inflation  
342 caused by inter-cohort overlap and relatedness in our simulations based on UK Biobank (European  
343 ancestry base and target samples) data (Figure 2). These simulations modelled a range of scenarios that  
344 varied trait heritability, prevalence, degree of overlap and combinations of overlap among cases and  
345 controls. For example, simulating quantitative traits with heritability 0.1, a base cohort of 250k samples,  
346 target cohort of 5000 samples, and degree of overlap 0.141 – in which all samples in the target data are  
347 also in the base GWAS – the mean  $\Delta R^2$  is  $-3.76 \times 10^{-4}$  (standard error:  $3.03 \times 10^{-4}$ ). Left unadjusted, the  
348 mean  $\Delta R^2$  is approximately 0.35 (standard error 0.00125), suggesting that EraSOR has removed the  
349 inflation introduced by sample overlap. A similar pattern of complete removal of the effects of sample  
350 overlap is observed for the quantitative traits across the full range of heritability and cohort sample sizes  
351 tested (Figure 2a).

352 EraSOR also performs extremely well for binary traits (Figure 2b, 2c, 2d). In binary traits with heritability  
 353 0.1, population prevalence 0.1, a base cohort of with 120k effective samples, and a target cohort of 5,000  
 354 effective samples, the mean  $R^2$  for the adjusted PRS in relation to case-only overlap is  $1.61 \times 10^{-4}$   
 355 (standard error =  $2.11 \times 10^{-4}$ ) (Fig 2b) and the mean  $R^2$  for the adjusted PRS in relation to control-only  
 356 overlap is  $-3.77 \times 10^{-5}$  (standard error =  $1.98 \times 10^{-4}$ ) (Fig 2c). On the other hand, when unadjusted, the mean  
 357  $R^2$  in relation to case only overlap is as high as  $0.161$  (standard error =  $8.93 \times 10^{-4}$ ), whereas the mean  
 358 is  $6.28 \times 10^{-3}$  (standard error =  $2.59 \times 10^{-4}$ ) in relation to control-only overlap.

359 While EraSOR effectively eliminates inflation caused by inter-cohort overlap in all simulation scenarios  
 360 tested in relation to heritable traits, false-positive results are still observed after EraSOR adjustment in  
 361 non-heritable traits when there is a large degree of overlap ( $> 0.29$ ). For non-heritable quantitative traits  
 362 with base cohorts of 120k samples and target cohorts of 10k samples, if all target samples are also present  
 363 in the base cohort, then we observe a false-positive rate of 87%, with a mean  $R^2$  of  $0.0028$  (standard  
 364 error =  $1.14 \times 10^{-4}$ ). This is likely caused by the fact that a key component of the mathematics underlying  
 365 the EraSOR algorithm (described by Eq. 11 in Methods) includes an estimate of  $h^2$  in its denominator.  
 366 Therfore, when the trait is non-heritable, Eq 9 may be unstable and lead to an error in the EraSOR  
 367 adjustment. However, we recommend that polygenic risk score analyses should not be performed on traits  
 368 with estimated  $h^2 < 0.05$  (see [1]) and, thus, in sufficiently powered applications of PRS, EraSOR should  
 369 have strong performance.

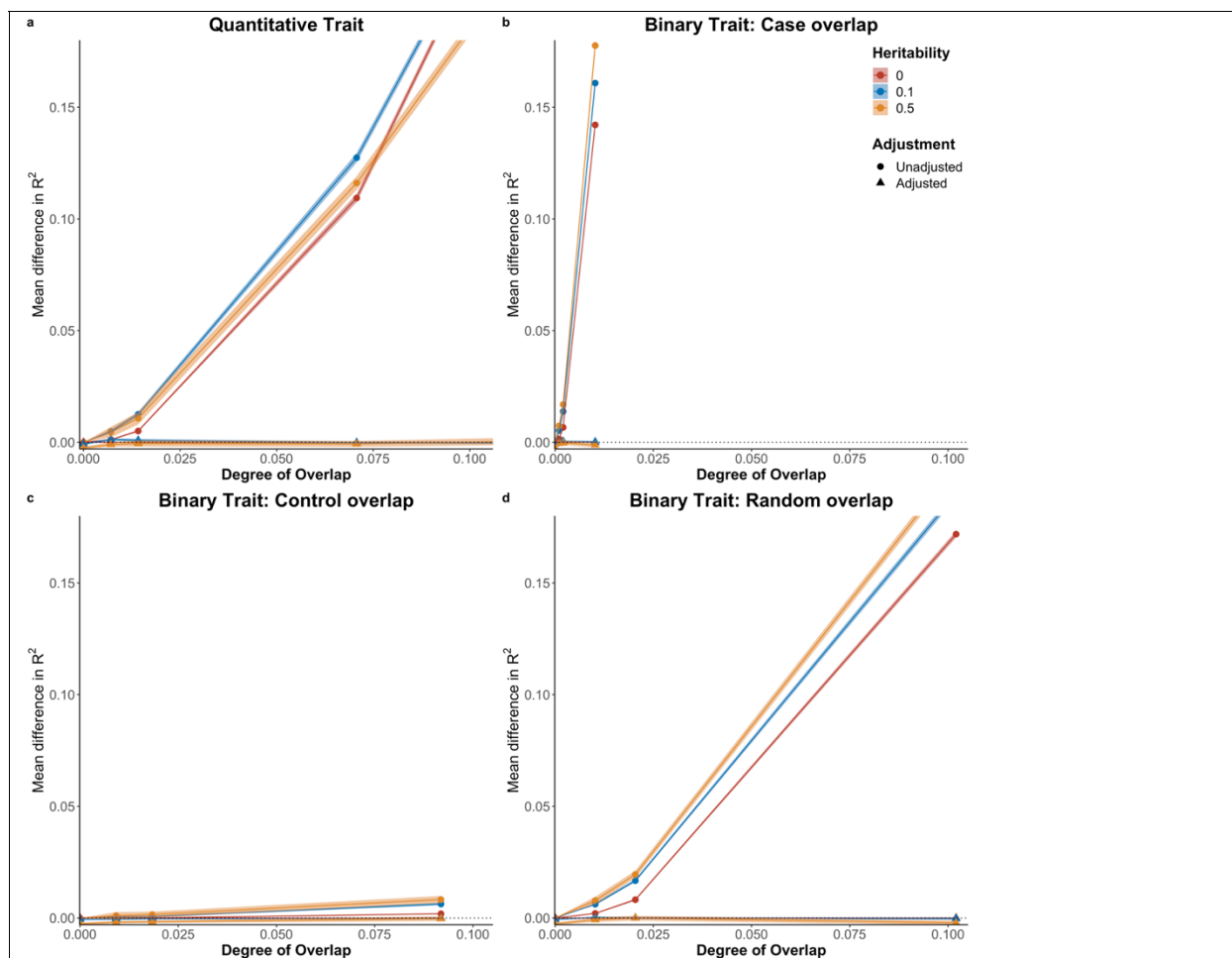


**Figure 2.** Comparing the performance of the PRS using the EraSOR adjusted summary statistics and the unadjusted summary statistics. The X-axis shows the degree of overlap, and the Y-axis shows the mean difference between the observed  $R^2$  and the expected  $R^2$ . Shaded area represents the 95% confidence interval (small on this scale). **a)** Performance in quantitative traits

with 250,000 samples in the base cohort and 5,000 samples in the target cohort; b) Performance in binary traits with prevalence of 0.1 and where overlap samples were ascertained for cases; c) ascertained for controls; d) or were randomly ascertained.

370

371 One of the main assumptions of EraSOR is that there is no environmental stratification ( $\sigma_s^2 = 0$ ). To  
372 investigate the robustness of EraSOR to model misspecification, we also performed simulations by  
373 incorporating UK Biobank samples with non-European ancestry and simulated different level of  
374 environmental stratification.

375 Overall, EraSOR is robust against model misspecification. For example, for quantitative traits with  
376 heritability of 0.1 and an environmental stratification of 0.3, the mean  $\Delta R^2$  is  $-2.7 \times 10^{-3}$  with standard error  
377 of  $6.96 \times 10^{-4}$  when the degree of overlap is 0.141 for target cohorts with 5000 samples and base cohorts  
378 with 250k samples. EraSOR performs equally well for quantitative traits with different heritability,  
379 different level of environmental stratifications and cohorts with different sample size and overlap (see  
380 Supplementary Fig. 3-6).

### 381 ***Robustness with diverse ancestry data***

382 While the  $F_{ST}$  between the European and non-European samples (see Methods) is high ( $F_{ST} = 0.018$ ), non-  
383 European samples accounts for only ~5% of the UK Biobank population. Our results might therefore be  
384 dominated by the European samples. To understand how EraSOR performs in a more heterogeneous  
385 dataset, additional simulations were performed using HapGen2 simulated genotype [22].

386 Using HapGen2 and the Finnish and Yoruban recombination maps from 1000 genome, we simulated  
387 180k “Finnish” and 180k “Yoruban” samples.  $F_{ST}$  estimation from PLINK between the two population is  
388 only 0.00638, much lower than the reported  $F_{ST} > 0.1$  African and European population [23]. This  
389 discrepancy is likely a result of the fact that the only difference in the simulations is the recombination  
390 map used (Supplementary Fig. 7) by HapGen2. Nonetheless, the HapGen2 simulation generates a dataset  
391 where the genetic signal is not dominated by one single population and allows us to better understand the  
392 performance of EraSOR in the presence of stratification.

393 Under the HapGen2 simulations, for quantitative traits with heritability 0.1, base cohort size of 250k,  
394 target cohort size of 5000, degree of overlap is 0.141 (all target samples also in the base cohort),  
395 environmental stratification 0.1, then the mean  $\Delta R^2$  for the adjusted PRS is  $-1.01 \times 10^{-3}$  (standard error =  
396  $9.41 \times 10^{-4}$ ); the mean  $\Delta R^2$  of the adjusted PRS is 0.0012 (standard error =  $8.17 \times 10^{-4}$ ) when the  
397 environmental stratification is 0.3, showing slight inflation. Nonetheless, when compared to the  
398 unadjusted PRS, which has mean  $\Delta R^2 = 0.225$ , the inflation of the adjusted PRS is small.

399 One potential reason for the robustness of EraSOR may be due to the simplistic population structure of  
400 the simulated genotype. As we simulated the environmental stratification according to the population  
401 label, it is possible that by adjusting for PCs, the environmental stratification was fully adjusted for.  
402 While it is highly unlikely that environmental stratification is orthogonal to population genetic structure,  
403 we performed an additional simulation in which the population label was randomly assigned to the  
404 simulated genotype. This ensured the simulation of environmental stratification independent of population  
405 genetic structure and, thus, should not be captured by PCA adjustment (see Supplementary Methods and  
406 Supplementary Fig. 8).

407 Even when environmental stratification is simulated independently of the population genetic structure,  
408 EraSOR adjustments are still robust to different environmental structure. For quantitative traits with

409 heritability of 0.1, base cohort size of 250k, target cohort size of 5,000 and environmental stratification of  
410 0.3, the mean for the adjusted PRS is  $-6.08 \times 10^{-4}$  (standard error =  $9.68 \times 10^{-4}$ ).

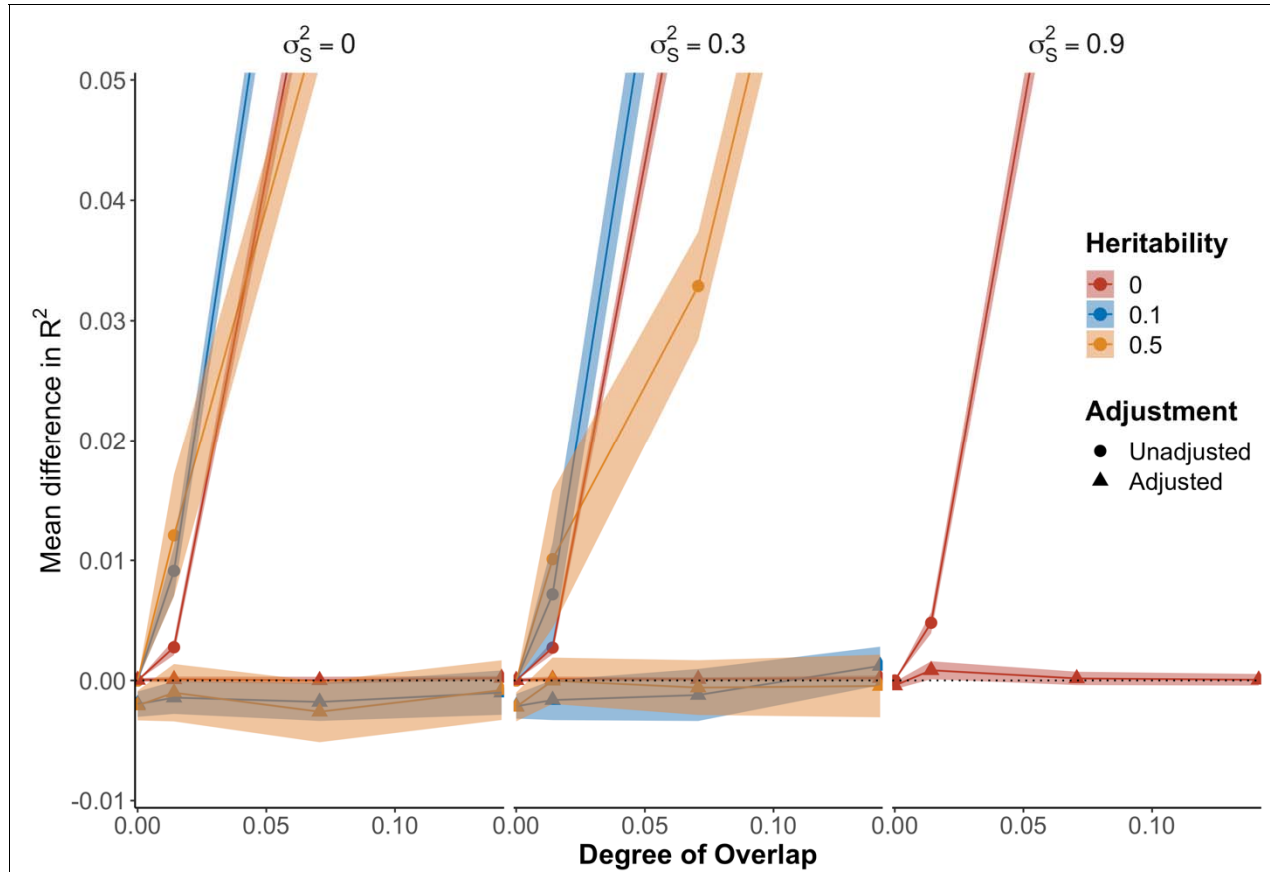


**Figure 3.** Performance of EraSOR from the HapGen2 simulation. Y-axis represents the mean difference between the observed  $R^2$  and the expected  $R^2$  and X-axis represents the degree of overlap. Range shows the 95% confidence interval. Based on simulation results, it seems like EraSOR are robust against different environmental stratification ( ).

411

## 412 **Discussion**

413 The recent advent of large-scale national and regional biobank projects, such as the UK Biobank [8],  
414 Japan Biobank [9] and FinnGen [11], have provided large resources of genotype-phenotype data ideal for  
415 conducting polygenic risk score analyses. However, this burgeoning generation of large data has led to an  
416 increased risk of inter-cohort sample overlap or relatedness, which can lead to inflated type 1 error. Due  
417 to privacy laws and practical concerns, it is usually impossible to identify overlapping samples or related  
418 samples across different cohorts. However, ideally researchers would be aware of the scale of the  
419 potential problem and have tools to mitigate against it. Therefore, here we reported on an investigation to  
420 evaluate the impact of inter-cohort sample overlap and relatedness in PRS analyses and developed a  
421 method to account for potential inter-cohort overlap and relatedness that does not require access to raw  
422 genotype data from the base GWAS.

423 We demonstrated that inter-cohort overlap results in a significant and often substantial inflation in the  
424 observed PRS-trait association, coefficient of determination ( $R^2$ ) and false-positive rate. This inflation can  
425 be high even when the absolute number of overlapping individuals is small if this makes up a notable  
426 fraction of the target samples. The inflation is noticeably more severe for binary traits with a small  
427 population prevalence when all the overlapping samples are cases. Therefore, PRS results will likely be  
428 misinterpreted unless inter-cohort sample overlap and close relatedness is properly accounted for.

429 Here, we developed the Erase Sample Overlap and Relatedness (EraSOR) method. EraSOR is designed to  
430 correct for inter-cohort sample overlap and relatedness using only summary statistics, without requiring  
431 any other information. The results of PRS analyses using EraSOR-adjusted GWAS results in the presence  
432 of sample overlap or relatedness was remarkably similar to those gained when the overlap was explicitly  
433 removed in most simulated conditions. EraSOR is also robust to mis-specification of the model, for  
434 example, when there is environmental stratification. While EraSOR does not fully adjust for the bias  
435 introduced by inter-cohort overlap for non-heritable traits when the degree of overlap is high, we  
436 recommend that researchers should not perform PRS analyses on non-heritable traits in any case [1].  
437 EraSOR performs well for the majority of simulation scenarios tested here, which we believe reflect a  
438 large fraction of PRS studies.

439 Theoretically, as  $\rho$  from the bivariate LD score regression is assumed to be the phenotypic correlation  
440 [18], we can apply EraSOR in situations where the base and target cohorts measure different phenotypes.  
441 Based on LeBlanc's equations [16], the spurious correlations caused by inter-cohort overlap and  
442 relatedness is a function of the phenotypic correlation. While this suggests that the impact of inter-cohort  
443 overlap and relatedness are likely to be smaller for cross-trait analyses, EraSOR adjustments may still be  
444 beneficial in these scenarios. Investigation of the performance of EraSOR in cross-trait analyses should be  
445 the subject of future work. Further research is also required to understand the performance and biases of  
446 EraSOR for applications in cross-trait studies and in its potential application to GWAS meta-analyses.

447 Our algorithm is not without any limitations. First, as EraSOR depends on the LD score intercept  
448 estimates for the adjustment, all assumptions of LD score regression also apply to EraSOR. For example,  
449 LD score regression assumes the level of genetic and environmental stratification is similar between the  
450 two cohorts [13], and if this assumption is violated, then it is likely that the bivariate LD score equation  
451 does not hold, which will lead to bias in EraSOR estimates. Moreover, due to reliance on LD score  
452 regression estimates, EraSOR only produces sufficiently accurate adjustments for application when both  
453 base and target cohorts have sample sizes greater than 1,000 and is only consistently accurate when both  
454 cohorts are greater than 5,000 samples. Nonetheless, despite its limitations, EraSOR is an ideal tool for  
455 application in settings in which there is known overlap in relation to large target samples and for  
456 sensitivity analyses in PRS studies. If the performance of PRS using the unadjusted and EraSOR adjusted  
457 summary statistics differs substantially, then this will act as a warning to the possible presence of inter-  
458 cohort overlap or close relatedness that should be adjusted for in order to obtain reliable PRS analysis  
459 results.

460 ***Availability of supporting source code and requirements***

Project Name	EraSOR
Project Homepage	<a href="https://choishingwan.gitlab.io/EraSOR/">https://choishingwan.gitlab.io/EraSOR/</a>
Programming Language	Python (version 3.0+)
License	GNU General Public License version 3.0 (GPLv3)
Any restrictions to use by non-academics	None

Simulation Scripts	<a href="https://gitlab.com/choishingwan/sample_overlap_paper">https://gitlab.com/choishingwan/sample_overlap_paper</a>
--------------------	---

## 461 ***Availability of supporting data and materials***

462 All code used for this paper is available at [https://gitlab.com/choishingwan/sample\\_overlap\\_paper](https://gitlab.com/choishingwan/sample_overlap_paper)  
463 and were implemented using nextflow (version 20.10.0 build 5430) [28].

## 464 ***Abbreviations***

465 PRS: polygenic risk score

## 466 ***Additional files***

467 Supplementary Table 1: Simulation results

## 468 ***Competing interests***

469 The authors declare that they have no competing interests.

## 470 ***Funding***

471 Medical Research Council FundRef identification ID: <http://dx.doi.org/10.13039/501100000265>  
472 MR/N015746/1 and the National Institute of Health (R01MH122866) to P.F.O. This report represents  
473 independent research partially funded by the National Institute for Health Research (NIHR) Biomedical  
474 Research Centre at South London and Maudsley NHS Foundation Trust and King's College London.  
475 Research reported in this paper was supported by the Office of Research Infrastructure of the National  
476 Institutes of Health under award number S10OD026880. The content is solely the responsibility of the  
477 authors and does not necessarily represent the official views of the National Institutes of Health, NHS, the  
478 NIHR or the Department of Health.

## 479 ***Authors' contributions***

480 Conceptualization, S.W.C. and P.F.O.; Methodology, S.W.C., T.S.H.M., C.H. and P.F.O.; Investigation,  
481 S.W.C.; Software, S.W.C.; Supervision, P.F.O.; Funding Acquisition, P.F.O.; Writing – Original Draft,  
482 S.W.C; Writing - Review and Edition, S.W.C., T.S.H.M., C.H. and P.F.O.;

## 483 ***Acknowledgements***

484        We thank the participants in the UK Biobank and the scientists involved in the construction of this  
485        resource. We thank Jonathan Coleman and Kylie Glanville for helpful discussions. This research has been  
486        conducted using the UK Biobank Resource under application 18177 (P.F.O.). This work was supported in  
487        part through the computational resources and staff expertise provided by Scientific Computing at the  
488        Icahn School of Medicine at Mount Sinai.

489

490

491 **Reference**

492 1. Choi SW, Mak TS-H, O'Reilly PF. Tutorial: a guide to performing polygenic risk score analyses. *Nat Protoc.* 2020; doi: 10.1038/s41596-020-0353-1.

494 2. Mavaddat N, Michailidou K, Dennis J, Lush M, Fachal L, Lee A, et al.. Polygenic Risk Scores for  
495 Prediction of Breast Cancer and Breast Cancer Subtypes. *Am J Hum Genet.* 2019; doi:  
496 10.1016/j.ajhg.2018.11.002.

497 3. Zhang J-P, Robinson D, Yu J, Gallego J, Fleischhacker WW, Kahn RS, et al.. Schizophrenia Polygenic  
498 Risk Score as a Predictor of Antipsychotic Efficacy in First-Episode Psychosis. *Am J Psychiatry.* 2019;  
499 doi: 10.1176/appi.ajp.2018.17121363.

500 4. Natarajan P, Young R, Stitziel NO, Padmanabhan S, Baber U, Mehran R, et al.. Polygenic Risk Score  
501 Identifies Subgroup with Higher Burden of Atherosclerosis and Greater Relative Benefit from Statin  
502 Therapy in the Primary Prevention Setting. *Circulation.* 2017; doi:  
503 10.1161/CIRCULATIONAHA.116.024436.

504 5. Mega JL, Stitziel NO, Smith JG, Chasman DI, Caulfield MJ, Devlin JJ, et al.. Genetic risk, coronary  
505 heart disease events, and the clinical benefit of statin therapy: an analysis of primary and secondary  
506 prevention trials. *The Lancet.* Elsevier; 2015; doi: 10.1016/S0140-6736(14)61730-X.

507 6. Pain O, Hodgson K, Trubetskoy V, Ripke S, Marshe VS, Adams MJ, et al.. Antidepressant Response in  
508 Major Depressive Disorder: A Genome-wide Association Study. *medRxiv.* Cold Spring Harbor  
509 Laboratory Press; 2020; doi: 10.1101/2020.12.11.20245035.

510 7. Dudbridge F. Power and Predictive Accuracy of Polygenic Risk Scores. *PLOS Genet.* 2013; doi:  
511 10.1371/journal.pgen.1003348.

512 8. Sudlow C, Gallacher J, Allen N, Beral V, Burton P, Danesh J, et al.. UK Biobank: An Open Access  
513 Resource for Identifying the Causes of a Wide Range of Complex Diseases of Middle and Old Age.  
514 *PLOS Med.* 2015; doi: 10.1371/journal.pmed.1001779.

515 9. Nagai A, Hirata M, Kamatani Y, Muto K, Matsuda K, Kiyohara Y, et al.. Overview of the BioBank  
516 Japan Project: Study design and profile. *J Epidemiol.* 2017; doi: 10.1016/j.je.2016.12.005.

517 10. Fan C-T, Lin J-C, Lee C-H. Taiwan Biobank: a project aiming to aid Taiwan's transition into a  
518 biomedical island. *Pharmacogenomics.* 2008; doi: 10.2217/14622416.9.2.235.

519 11. FinnGen. FinnGen Documentation of R3 release.

520 12. Sullivan PF, Agrawal A, Bulik CM, Andreassen OA, Børglum AD, Breen G, et al.. Psychiatric  
521 Genomics: An Update and an Agenda. *Am J Psychiatry.* 2018; doi: 10.1176/appi.ajp.2017.17030283.

522 13. Yengo L, Sidorenko J, Kemper KE, Zheng Z, Wood AR, Weedon MN, et al.. Meta-analysis of  
523 genome-wide association studies for height and body mass index in ~700000 individuals of European  
524 ancestry. *Hum Mol Genet.* 2018; doi: 10.1093/hmg/ddy271.

525 14. Global Lipids Genetics Consortium, Willer CJ, Schmidt EM, Sengupta S, Peloso GM, Gustafsson S,  
526 et al.. Discovery and refinement of loci associated with lipid levels. *Nat Genet.* 2013; doi:  
527 10.1038/ng.2797.

528 15. Wray NR, Yang J, Hayes BJ, Price AL, Goddard ME, Visscher PM. Pitfalls of predicting complex  
529 traits from SNPs. *Nat Rev Genet*. 2013; doi: 10.1038/nrg3457.

530 16. LeBlanc M, Zuber V, Thompson WK, Andreassen OA, Frigessi A, Andreassen BK, et al.. A  
531 correction for sample overlap in genome-wide association studies in a polygenic pleiotropy-informed  
532 framework. *BMC Genomics*. 2018; doi: 10.1186/s12864-018-4859-7.

533 17. Bulik-Sullivan BK, Loh P-R, Finucane HK, Ripke S, Yang J, Schizophrenia Working Group of the  
534 Psychiatric Genomics Consortium, et al.. LD Score regression distinguishes confounding from  
535 polygenicity in genome-wide association studies. *Nat Genet*. 2015; doi: 10.1038/ng.3211.

536 18. Bulik-Sullivan B, Finucane HK, Anttila V, Gusev A, Day FR, Loh P-R, et al.. An atlas of genetic  
537 correlations across human diseases and traits. *Nat Genet*. 2015; doi: 10.1038/ng.3406.

538 19. Choi SW. GreedyRelated: Script for greedily remove related samples.

539 20. Falconer DS. Introduction to quantitative genetics. New York,: Ronald Press Co;

540 21. Willer CJ, Li Y, Abecasis GR. METAL: fast and efficient meta-analysis of genomewide association  
541 scans. *Bioinformatics*. 2010; doi: 10.1093/bioinformatics/btq340.

542 22. Su Z, Marchini J, Donnelly P. HAPGEN2: simulation of multiple disease SNPs. *Bioinforma Oxf Engl*.  
543 2011; doi: 10.1093/bioinformatics/btr341.

544 23. Auton A, Abecasis GR, Altshuler DM, Durbin RM, Abecasis GR, Bentley DR, et al.. A global  
545 reference for human genetic variation. *Nature*. Nature Publishing Group; 2015; doi: 10.1038/nature15393.

546 24. Abraham G, Qiu Y, Inouye M. FlashPCA2: principal component analysis of Biobank-scale genotype  
547 datasets. *Bioinformatics*. 2017; doi: 10.1093/bioinformatics/btx299.

548 25. Chang CC, Chow CC, Tellier LC, Vattikuti S, Purcell SM, Lee JJ. Second-generation PLINK: rising  
549 to the challenge of larger and richer datasets. *GigaScience*. 2015; doi: 10.1186/s13742-015-0047-8.

550 26. Choi SW, O'Reilly PF. PRSice-2: Polygenic Risk Score software for biobank-scale data.  
551 *GigaScience*. 2019; doi: 10.1093/gigascience/giz082.

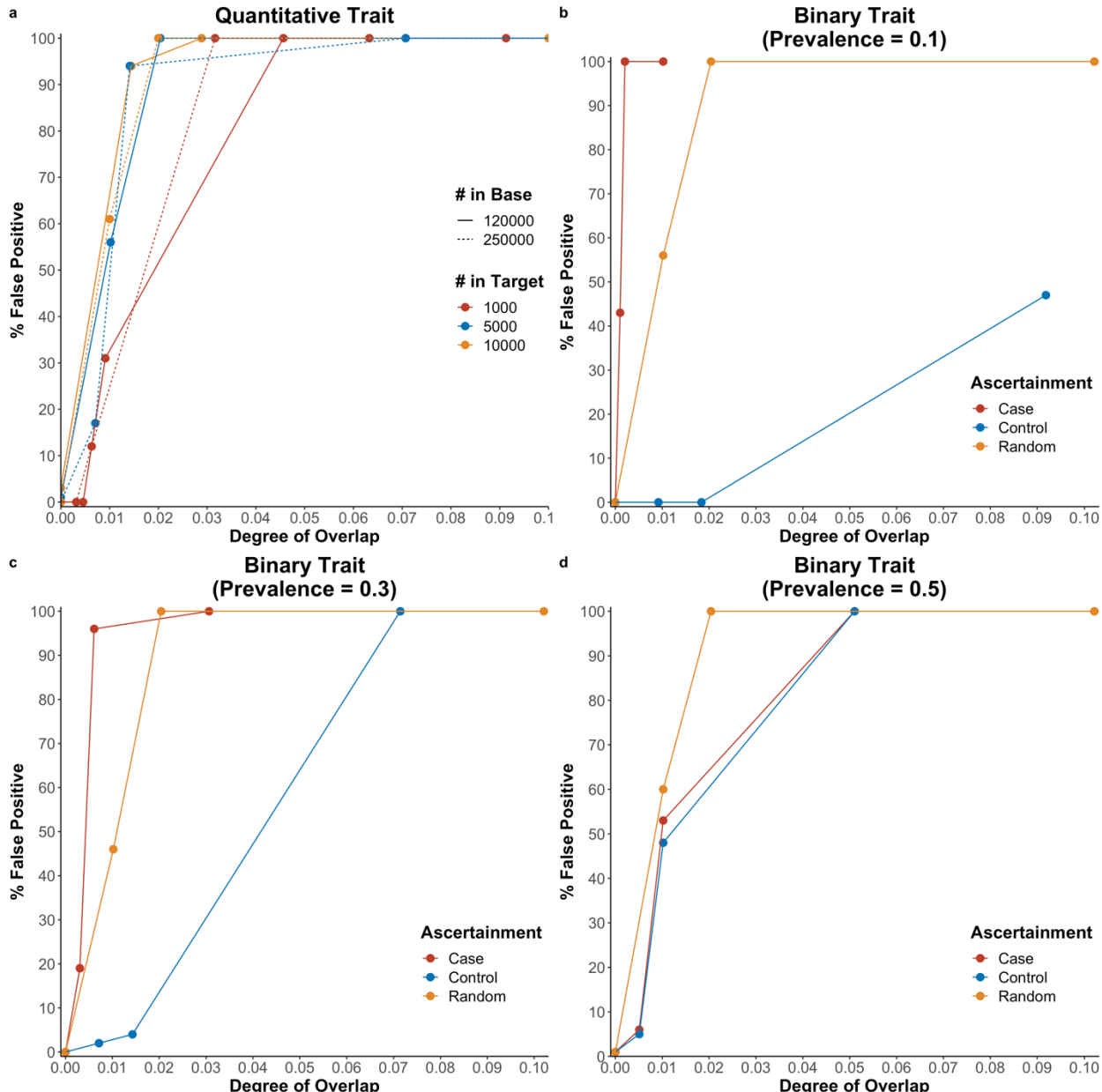
552 27. Euesden J, Lewis CM, O'Reilly PF. PRSice: Polygenic Risk Score software. *Bioinformatics*. 2015;  
553 doi: 10.1093/bioinformatics/btu848.

554 28. Di Tommaso P, Chatzou M, Floden EW, Barja PP, Palumbo E, Notredame C. Nextflow enables  
555 reproducible computational workflows. *Nat Biotechnol*. 2017; doi: 10.1038/nbt.3820.

556

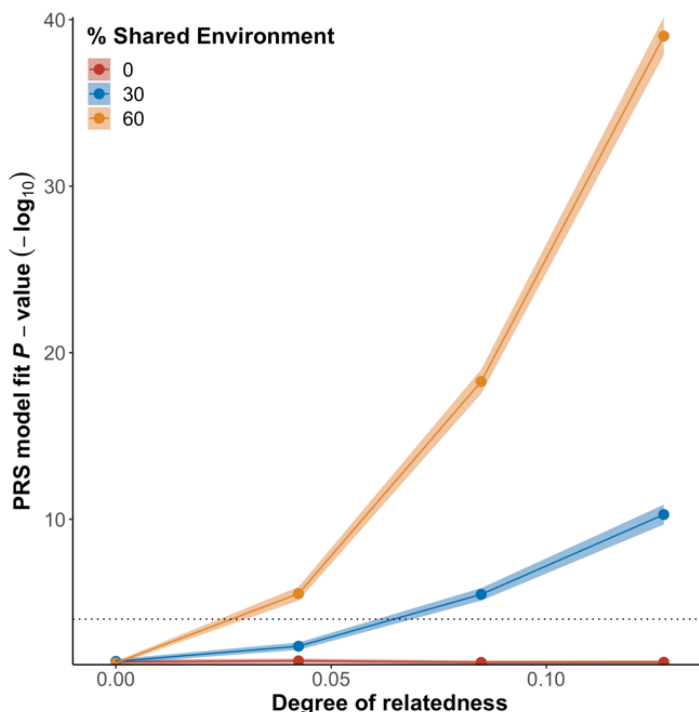
557

558 **Supplementary Materials**



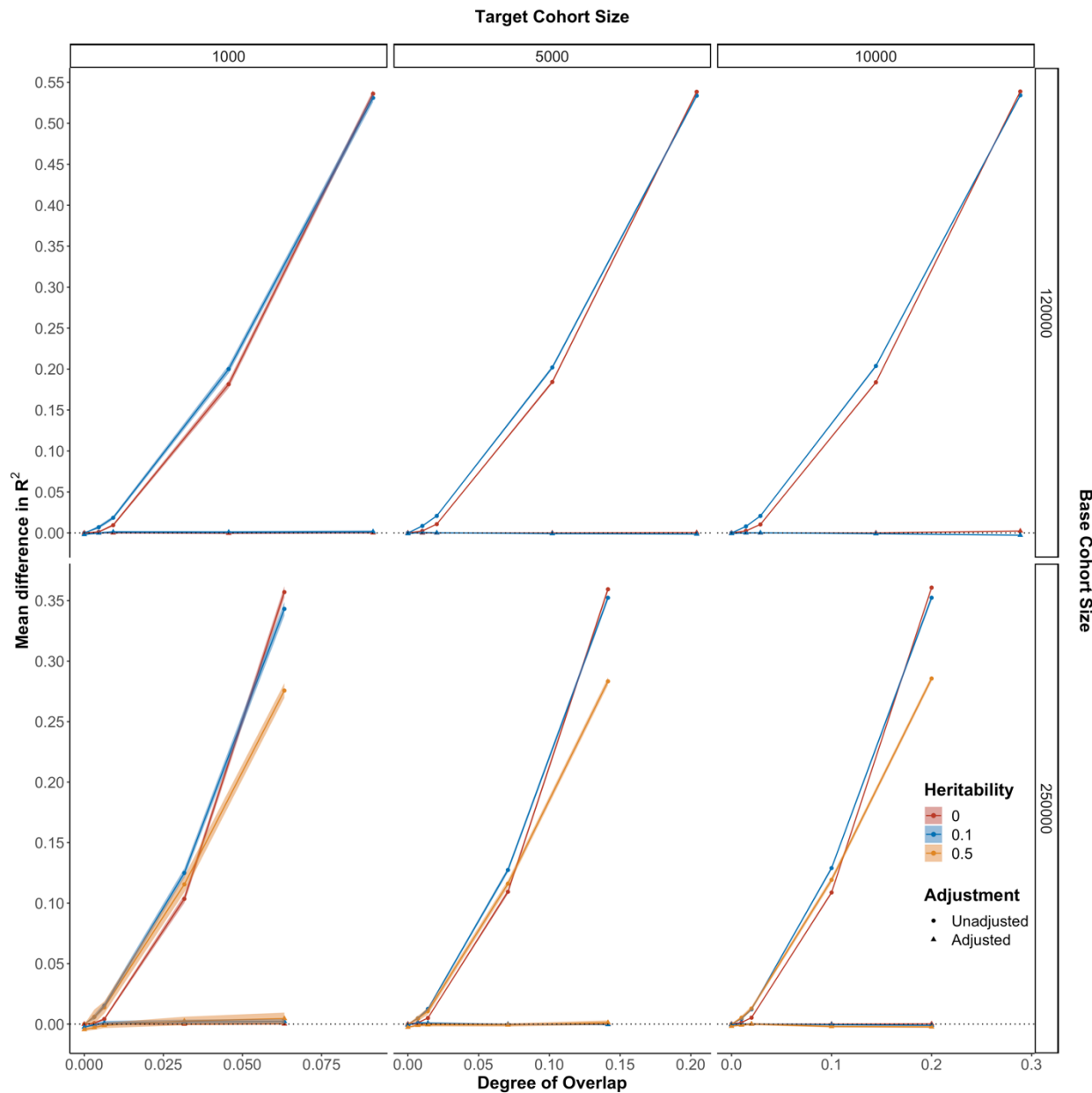
559

560 **Supplementary Figure 1.** False positive rate corresponding to different level of sample overlap. Non-  
561 heritable phenotypes were simulated. X axis shows the degree of overlap, calculated as  $\frac{\text{Number of overlapping variants}}{\text{Number of variants in the base population}}$  and the Y-  
562 axis shows the percentage of false positive (PRS P-value  $< 1 \times 10^{-4}$ ). **a)** Quantitative traits with different  
563 cohort sizes **b)** Binary traits with population prevalence of 0.1 **c)** Binary traits with population prevalence  
564 of 0.3 **d)** Binary traits with population prevalence of 0.5.



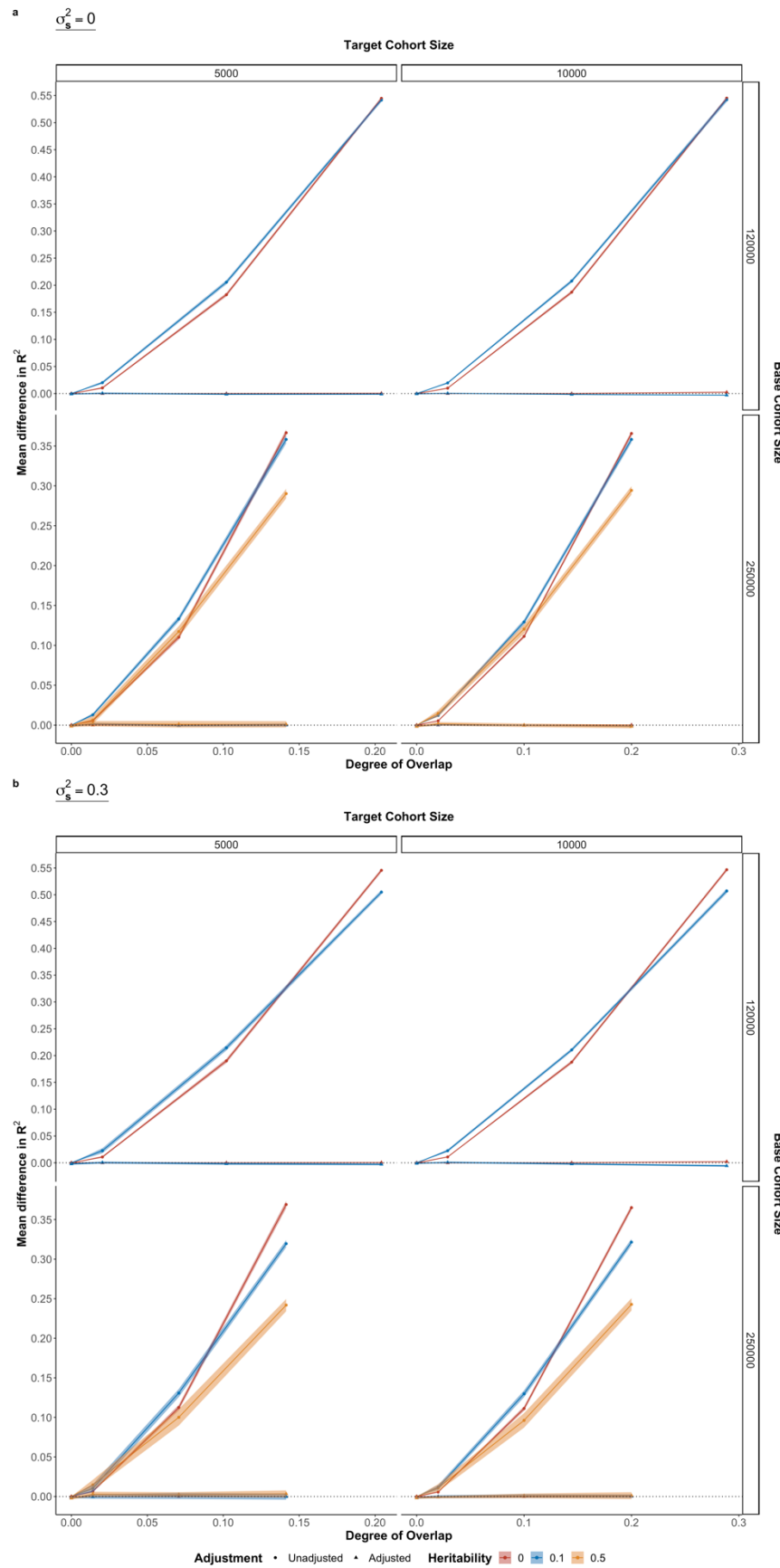
565

566 **Supplementary Figure 2.** Effect of sample relatedness on performance of PRS for non-heritability  
567 phenotypes. The dotted line represents the significant threshold i.e.,  $p$ -value  $< 1 \times 10^{-4}$ . Y-axis represents  
568 the  $-\log_{10}$  transformed  $p$ -value of association between the PRS and the phenotype; the X-axis represents  
569 the degree of relatedness between the target cohort and the base cohort, calculated  $\frac{n}{N}$  where  $n$  is the  
570 number of samples in the target cohort that are first degree relatives to sample in the base cohorts. Shaded  
571 area represent the 95% confidence interval.

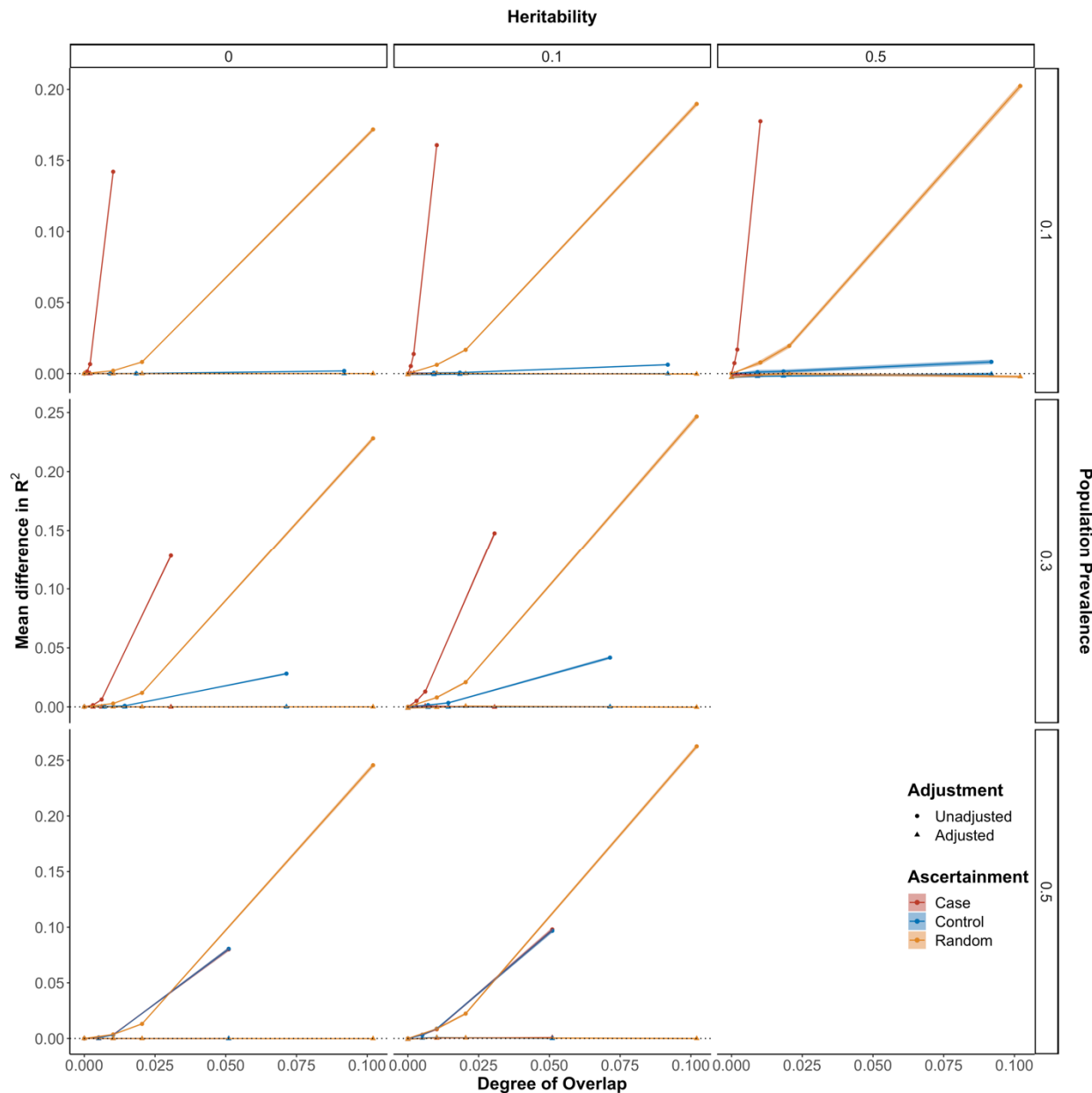


572

573 **Supplementary Figure 3.** Comparing the performance of PRS using the EraSOR adjusted summary  
574 statistics and the unadjusted summary statistics for quantitative trait without population stratification. The  
575 X-axis shows the degree of overlap, and the Y-axis shows the mean difference between the observed  $R^2$   
576 and the expected  $R^2$ . Mean difference in  $R^2 = 0$  is represented by the black dotted line. Each row  
577 corresponds to different base cohort sizes, each column corresponds to different target cohort size and  
578 different colors correspond to different trait heritability. Performance of the adjusted PRS is indicated  
579 with triangle and performance of the unadjusted PRS is indicated with circle. Shaded area represents the  
580 95% confidence interval, which tends to be small.



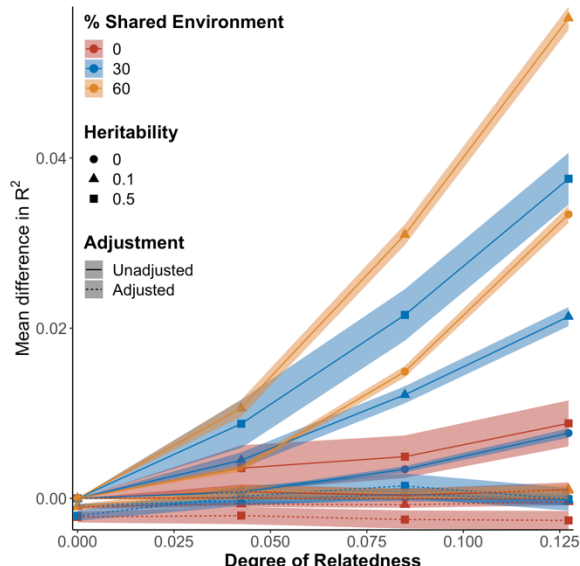
582 **Supplementary Figure 4.** Comparing the performance of PRS using the EraSOR adjusted summary  
583 statistics and the unadjusted summary statistics for quantitative trait when there are population  
584 stratifications. Samples from non-European ancestries were included in this analysis. Different level of  
585 environmental stratifications was simulated: **a)** no environmental stratification **b)** environmental  
586 stratification = 0.3. Shaded area represents the 95% confidence interval, with different colours represent  
587 different simulated heritability. Results of the unadjusted PRS were represented with circle, while results  
588 of the adjusted PRS were represented with triangle.



589

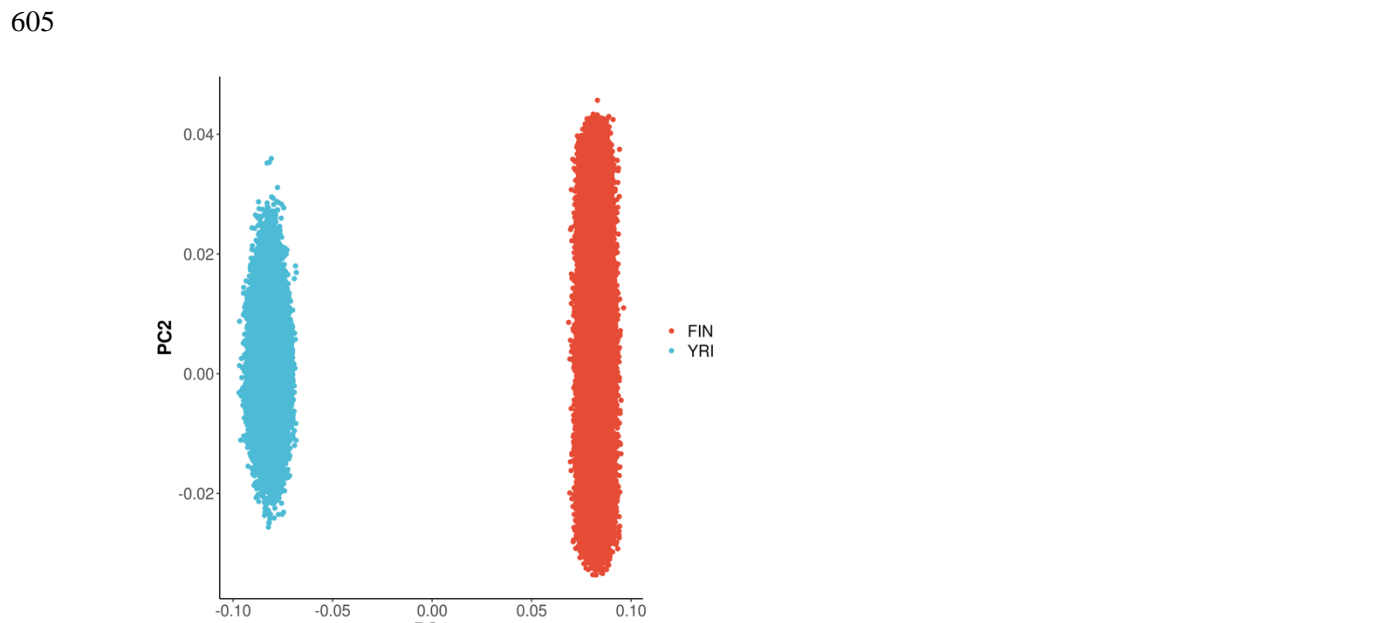
590 **Supplementary Figure 5.** Comparing the performance of PRS using the EraSOR adjusted summary  
591 statistics and the unadjusted summary statistics for binary trait analyses. The X-axis shows the degree of  
592 overlap, and the Y-axis shows the mean difference between the observed  $R^2$  and the expected  $R^2$ . Mean  
593 difference in  $R^2 = 0$  is represented by the black dotted line. Each row corresponds to different trait  
594 heritability, each column corresponds to different population prevalence and colors were used to represent

595 different ascertainment of the overlapped samples. Performance of the adjusted PRS is indicated with  
596 triangle and performance of the unadjusted PRS is indicated with circle. Shaded area represents the 95%  
597 confidence interval, which tends to be small.



598

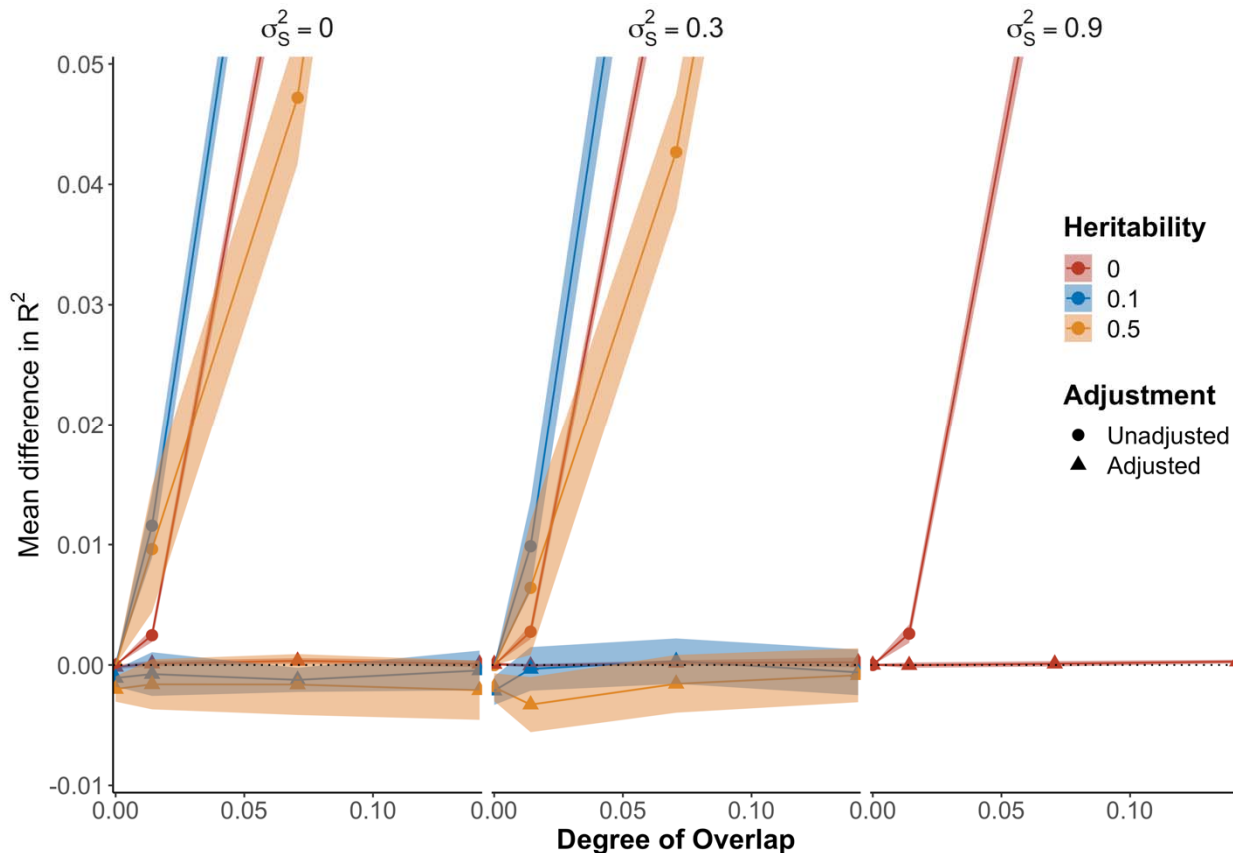
599 **Supplementary Figure 6.** Performance of EraSOR when adjusting for related samples between the target  
600 cohort and the base cohort. The X-axis shows the degree of overlap, and the Y-axis shows the mean  
601 difference between the observed  $R^2$  and the expected  $R^2$ . Shaded areas represent the 95% confidence  
602 interval. Different colours correspond to the amount of shared environmental contribution, and the shapes  
603 represents the heritability. Performance of EraSOR adjusted PRS are represented with the dotted line, and  
604 the performance of the unadjusted PRS are represented with the solid line.



606

607 **Supplementary Figure 7.** Principle Component plot for HapGen2 simulated data. Samples from the two  
608 populations were clearly separated by PC1, whereas PC2 does not contribute to the separation, suggesting

609 that the simulated population structure might be much simpler than what would otherwise observe in real  
610 data.



611  
612 **Supplementary Figure 8.** Performance of EraSOR adjusted PRS (triangle) against unadjusted PRS  
613 (circle) in HapGen2 simulations where phenotypes were stratified with agnostic environmental  
614 stratifications. The X-axis shows the degree of overlap, and the Y-axis shows the mean difference  
615 between the observed  $R^2$  and the expected  $R^2$ . Shaded area shows the 95% confidence interval. Our result  
616 suggest EraSOR are robust against different environmental stratification ( ) even when they are agnostic  
617 to the principal components.

## 618 *Supplementary Methods*

### 619 *Simulate environmental stratifications agnostic to population structures*

620 Similar to the main HapGen2 simulation, we used HapGen2 [22] to simulate 180k Yoruban and 180k  
621 Finnish samples using recombination maps from the 1000 Genomes Project [23]. 500 “Finnish” samples  
622 and 500 “Yoruban” samples were selected to calculate the LD scores using LDSC (v1.0.1) and flashPCA  
623 (v2.0) [24] was used to calculate the first 15 PCs of the data. — and — were randomly  
624 assigned to each individual, disregarding their simulated population.

625 The entire set of simulations were repeated 25 times.

626